

Experimental study of the onset of nucleate boiling in vertical helically-coiled tubes

Kong Lingjian¹ Han Jitian² Chen Changnian² Liu Zhigang¹

(¹Energy Research Institute of Shandong Academy Sciences, Jinan 250014, China)

(²School of Energy and Power Engineering, Shandong University, Jinan 250061, China)

Abstract: The experiments of the onset of nucleate boiling using R134a as working fluid were conducted in vertical helically-coiled tubes. The experiments were carried out with a range of pressure from 450 to 850 kPa, inlet subcooling from 4.7 to 15.0 °C, heat flux from 0.11 to 8.9 kW/m² and mass flux from 218.2 to 443.7 kg/(m² · s). The heat flux, superheat and temperature undershoot at the ONB are analyzed in vertical helically-coiled tubes. Also, the effects of mass flux, system pressure, inlet subcooling and geometric parameters on the ONB are studied. The results demonstrate that the inception heat flux and superheat increase with increasing mass flux and inlet subcooling, but decrease with increasing system pressure and helix diameter. The pitch of the helical coil has a slight effect on the wall superheat and heat flux at the ONB. The correlation of heat flux at the ONB of subcooled flow boiling in helical coil is developed based on the experimental data, and it shows a good agreement with the experimental data.

Key words: two-phase flow; subcooled flow boiling; onset of nucleate boiling; helical coil

DOI:10.3969/j.issn.1003-7985.2018.03.017

Subcooled flow boiling is characterized by boiling occurring near the heated wall while the bulk liquid temperature remains below its saturation temperature. The partitioning of subcooled flow boiling begins with onset of nucleate boiling (ONB), which marks the boundary between single and two-phase flow. The ONB indicates the location in which the vapor can first exist in a stable state on the heated surface.

Due to its complexity and importance, the characteristics of the ONB were investigated theoretically and experimentally by many researchers. The minimum superheat criterion for the boiling inception was first proposed by Hsu^[1]. According to his criterion, bubbles could be generated only if the temperature of the neighboring liquid

exceeds the saturation temperature. Kandlikar et al.^[2] calculated the temperature of the stagnation point around the bubble, which was used as the minimum temperature in the ONB criterion. Basu et al.^[3] proposed a correlation for calculating the heat flux and wall superheat at the ONB, which includes the effects of flow rate, subcooling and contact angle on the ONB. The characteristics of the ONB were investigated in narrow channels^[4], internal combustion engines^[5] and rod bundle channel^[6].

Due to the compactness in volume and high efficiency of heat transfer, the helically-coiled tube has attained considerable attention in research and practical application^[7-8]. However, it is evident that the onset of subcooled flow boiling in helical coils remains less explored based on the available literature. Kong et al.^[9] investigated the characteristics of the ONB in horizontal coils. The objective of the continuing investigation is to study the ONB in vertical helically-coiled tubes with R134a. The effects of experimental parameters on the ONB are investigated in detail. Meanwhile, the correlation of heat flux at the ONB is developed by means of multiple nonlinear regression analyses, which is applied to the vertical helically-coiled tube.

1 Experimental Set-Up and Data Acquisition

1.1 Experimental set-up

As shown in Fig. 1, the experimental set-up is employed to study the onset of subcooled flow boiling in vertical helically-coiled tubes for the upward flow of R134a. The experimental set-up is composed of working (R134a) and cooling (30% CaCl₂ solution) loops, the electric heating system and data acquisition system. The R134a, being pumped from the receiver by a metering pump, flowed successively through the mass flow-meter, sight glass, preheater, test section, and finally the condenser. The cooling loop, which is comprised of a chiller, cooling tower and condenser, is used to condense and further subcool R134a. The test section and preheater are directly heated by the DC power supplies, respectively.

During the experiment, the mass flux G , heat flux q'' , and inlet temperature T and pressure P of the test section can be regulated independently. The mass flux of R134a can be varied by changing the effective stroke length of the metering pump. At the same time, the flow rate of R134a

Received 2017-12-21, **Revised** 2018-04-15.

Biographies: Kong Lingjian (1986—), male, doctor; Han Jitian (corresponding author), male, doctor, professor, jthian@sdu.edu.cn.

Foundation items: The National Natural Science Foundation of China (No. 50776055, 51076084), the Natural Science Foundation of Shandong Province (No. ZR2016YL005).

Citation: Kong Lingjian, Han Jitian, Chen Changnian, et al. Experimental study of the onset of nucleate boiling in vertical helically-coiled tubes[J]. Journal of Southeast University (English Edition), 2018, 34 (3): 402–407. DOI:10.3969/j.issn.1003-7985.2018.03.017.

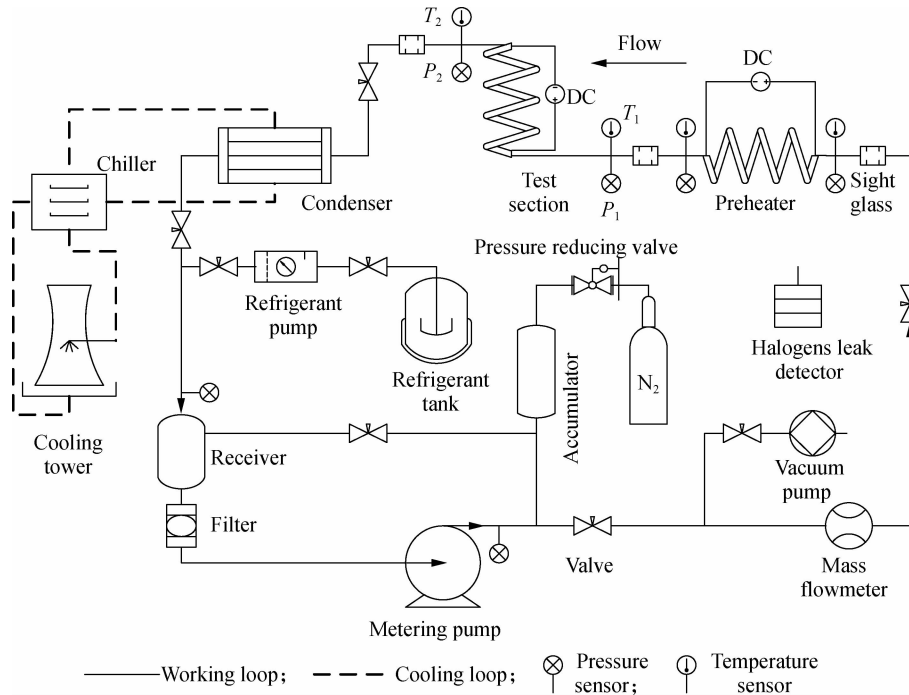


Fig. 1 Schematic diagram of the experimental set-up

is measured by a Coriolis mass flow meter. The heat fluxes of preheater and test section are controlled by setting the output voltage of the DC power supplies, respectively. The inlet temperature of R134a can be adjusted by the heat flux of preheat and cooling capacity of the condenser, which is determined by the flow rate and temperature of the coolant. The inlet pressure of the test section can be regulated by the pressure valve at the downstream of the test section. The inlet temperature and pressure can be measured by the T-type sheathed thermocouple and pressure sensor which are installed at the inlet of the test section, respectively. Moreover, the accumulator is used to reduce the flow rate and pressure fluctuations during the experiment. At the beginning of the experiment, the system parameters such as mass flux, inlet pressure and temperature are adjusted to the preset value. Then, the heat flux is increased gradually at a fixed rate until the ONB occurs on the upstream of the test section. All tests are performed under steady-state conditions.

1.2 Test section

As shown in Fig. 2, the helical coil is positioned vertically (see Fig. 2(a)), which is made of a 06Cr19Ni10 stainless steel tube. In order to study the effects of the geometric parameters of the helical coil on the ONB, four helical coils are tested and the geometric parameters are provided in Tab. 1. As shown in Fig. 2, D_c is the diameter of the coil; d_p is the pitch of the coil; L is the heated length; d_o and d_i are the outer and inner diameter of the test tube, respectively.

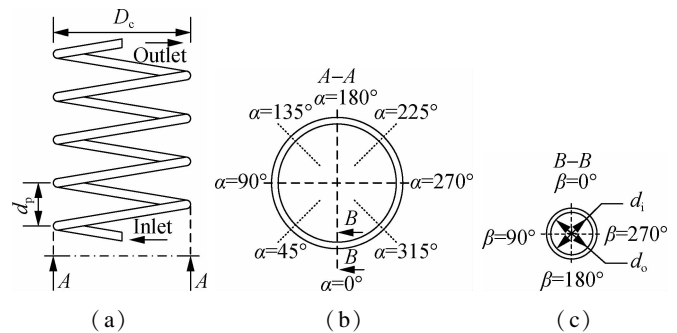


Fig. 2 Schematic of test section and installation of thermocouples. (a) Vertical coil; (b) Bottom view of the helical coil; (c) Cross section of the test tube

Tab. 1 Geometric parameters of the test section mm

Coil	Outer diameter d_o	Inner diameter d_i	Coil diameter D_c	Helical pitch d_p	Length L
Coil1	10.0	8.0	380	120	4 797
Coil2	10.0	8.0	380	80	4 784
Coil3	10.0	8.0	380	40	4 776
Coil4	10.0	8.0	220	80	2 782

The outer wall temperature is measured by the attached thermocouples and the installation positions are shown in Figs. 2(b) and (c). The location is denoted by angle α and β which are the angular position of the coil and cross-section, respectively. Starting from $\alpha = 0^\circ$, eight positions with 45° apart are selected as the measuring cross-section (see Fig. 2(b)). At each cross-section, four thermocouples are installed around the tube circumference evenly at $\beta = 0^\circ, 90^\circ, 180^\circ$ and 270° (see Fig. 2(c)). For each turn of the coil, the temperature of the tube wall is measured by 32 thermocouples. The test section is well

insulated by the polyethylene insulation layer with 20 mm in thickness. The total heat loss of the test section is measured experimentally to be less than 4.5%.

1.3 Data acquisition

All the signals of the system parameters are collected by the Agilent 34980A data acquisition system. The thermodynamic and transport properties of R134a used in the experimental investigation are calculated by REFPROP 9.0 of NIST. Using resistive heating, the preheater and test section are heated with the uniform heat flux by ignoring the change of the resistance with temperature. The heat flux added to the coil, q'' , is calculated by

$$q'' = \frac{\eta U^2}{\pi d_i L R} \quad (1)$$

where η is the thermal efficiency; U and R are the applied voltage and electrical resistance of the test tube, respectively.

The uncertainties of the experimental results are estimated by the methods proposed by Moffat^[10], and the maximum relative uncertainties are listed in Tab. 2. The directly measured parameters in experiments include length, pressure and temperature. The uncertainties of these parameters are calculated by the instructions of measurement equipment. Based on the root-sum-square method, the uncertainty of indirect measurement can be calculated by

$$\frac{\delta f}{f_{\min}} = \left[\sum_{i=1}^n \left(\frac{\partial f}{\partial x_i} \delta x_i \right)^2 \right]^{0.5} \frac{1}{f_{\min}} \quad (2)$$

The partial derivative of f in relation to x_i is the sensitivity coefficient for the result f in relation to the measurement x_i , and f_{\min} is the minimum in the operating range.

Tab. 2 Summary of the uncertainty analysis

Parameter	Operating range	Uncertainty/%
Tube diameter/mm	8.0 to 10.0	0.25
Pitch/mm	40.0 to 120.0	0.25
Tube length/mm	220 to 380	0.23
Coil diameter/mm	2 782 to 4 797	0.23
Pressure/kPa	450 to 850	0.89
Temperature/°C	5.1 to 32.1	5.55
Mass flux/ ($\text{kg} \cdot \text{m}^{-2} \cdot \text{s}^{-1}$)	218.2 to 443.7	4.55
Heat flux/($\text{kW} \cdot \text{m}^{-2}$)	0.11 to 8.9	1.72

2 Results and Discussion

The experiments are carried out at a pressure ranging from 450 to 850 kPa, inlet subcooling (ΔT_{sub}) from 4.7 to 15.0 °C, heat flux from 0.11 to 8.9 kW/m² and mass flux from 218.2 to 443.7 kg/(m² · s). The boiling curves of subcooled flow boiling in vertical helically-coiled tubes are analyzed. Moreover, the effects of pressure, subcooled temperature, mass flux and geometric pa-

rameters on the ONB are presented in detail. Finally, the correlation for predicting the heat flux at the ONB, which is suitable for vertical coils, is proposed based on the experimental data. To eliminate the entrance and exit effects, the experimental data in the second or third turn of the helically-coiled tube is selected to clarify the characteristics of the ONB.

2.1 Determination of the ONB

As the typical phenomenon of the ONB, the wall temperature will deviate from the linear growth process due to the change of the heat transfer mechanism^[3], which is the criterion for the occurrence of the ONB in the paper. The boiling curves measured at the coil position of $\alpha = 315^\circ$ with $\beta = 0^\circ, 90^\circ, 180^\circ$ and 270° are shown in Fig. 3, respectively. For single-phase flow, the wall temperature increases proportionally by increasing the heat flux gradually. When the wall temperature is high enough, bubble nucleation occurs and there is a significant temperature undershoot at the ONB. The temperature undershoot at the ONB results from the variation of heat transfer mechanism which changes from single phase forced convection to nucleate boiling.

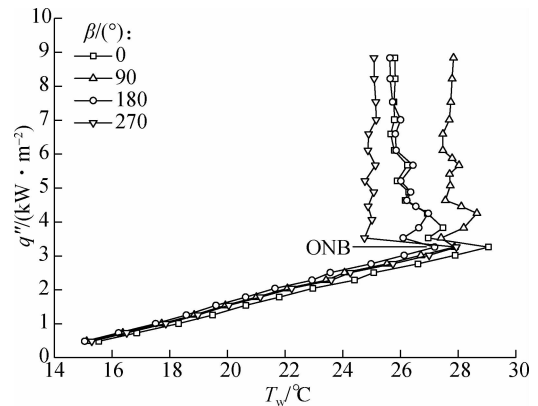


Fig. 3 Subcooled flow boiling curves in the vertical helically-coiled tube

The discussion here is focused on single phase flow. As shown in Fig. 3, the temperature distribution tested at the position of $\alpha = 315^\circ$ is manifested at $P = 650$ kPa, $G = 220.9$ kg/(m² · s) and $\Delta T_{\text{sub}} = 9.8$ °C. The temperature of the inner side ($\beta = 0^\circ$) is higher than that of the outer side ($\beta = 180^\circ$), while the temperature of the upper side ($\beta = 90^\circ$) is slightly lower than that of the lower side ($\beta = 270^\circ$) and the temperature values in between the inner and outer side before the ONB occurs. The temperature distribution of the cross-section is attributed to the secondary flow and velocity profile of the main flow. For simplification, the velocity distributions of the main flow and secondary flow are schematically shown in Fig. 4, which were first proposed by McConalogue and Srivastava^[11]. First, the velocity of the main flow near the outer side is faster than that of the inner side, which enhances the heat transfer of the outer side. Secondly, the

secondary flow perpendicular to the axis is induced by centrifugal force. With the influence of the secondary flow, the R134a near the upper and lower sides is moving inwards while that in the central plane is moving outwards. As a result, the temperature difference of the outer side is larger than that of the inner side. Based on the description above, the heat transfer in the outer side is better than that in the inner side and thus results in the temperature of the outer side being lower than the inner side. The circumferential non-uniformity of the wall temperature becomes obvious with the increase in heat flux in the single-phase regime.

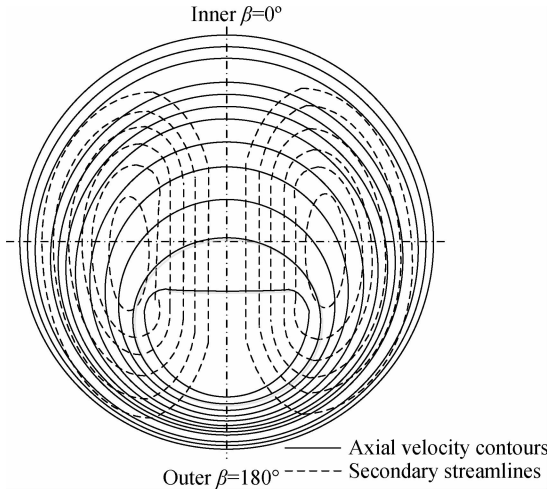


Fig. 4 Schematic representation of axial velocity contours and secondary streamlines

The ONB is marked in Fig. 3. It is noted that there is not much difference in the heat flux at the ONB for different angle β . However, a notable difference exists in the wall superheat ($T_{\text{sat}} = T_w - T_{\text{sat}}$) at the ONB for different angle β of the same cross-section. At the point of the ONB, the wall superheat of the inner side is 1.6 times that of the outer side, and the superheats of upper and lower sides are all 3.7°C . The characteristics of the wall superheat at the ONB are closely related to the distribution of wall temperature in the single phase flow. It is also noted from Fig. 3 that the temperature undershoots of this cross-section can be as high as 3.2°C for the upper side which is 5.4 times larger than the lower side. The temperature undershoot difference between the upper and lower sides is attributed to the heat transfer characteristics in subcooled flow boiling. With the influence of the bubble behavior, the heat transfer enhancement of the upper side enlarges the temperature undershoot. As a result of the distribution of wall temperature in the single phase flow, the temperature undershoot of the inner side is almost twice as large as the outer side.

2.2 Parametric effects on the ONB

To clarify the effects of experimental parameters on the ONB, the data is presented in terms of imposing heat flux

versus mean wall superheat of the cross-section.

As shown in Fig. 5(a), the effect of the inlet subcooling on the ONB is manifested for $\Delta T_{\text{sub}} = 4.7, 9.8$ and 15.0°C at $G = 219.4 \text{ kg}/(\text{m}^2 \cdot \text{s})$ and $P = 650 \text{ kPa}$ in No. 1 coil at the cross-section of $\alpha = 0^\circ$. The results indicate that the higher the subcooling, the higher the wall superheat and heat flux needed to initiate the nucleate boiling on the heated wall. It is also noted that a substantial increase in the temperature undershoot occurs when the subcooling is raised from 4.7 to 15.0°C . It is evident that the heat transfer between the heated wall and the liquid is enhanced at a higher inlet subcooling in the single phase flow. As a result, the heat flux and temperature undershoot at the ONB are higher at a specified wall superheat for higher liquid subcooling.

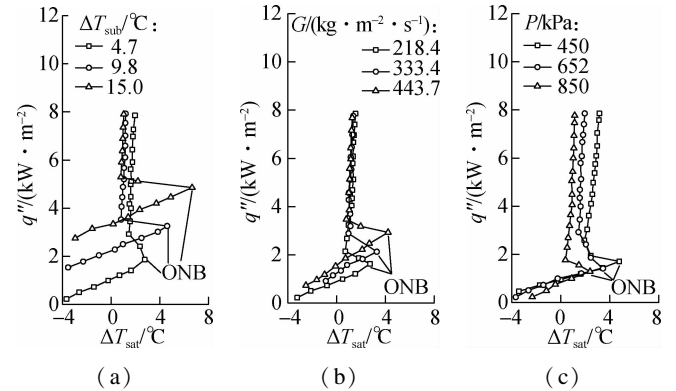


Fig. 5 Dependence of the ONB on system parameters. (a) Subcooling; (b) Mass flux; (c) Pressure

The effect of mass flux on the ONB is tested in No. 1 coil at $\alpha = 135^\circ$ for $G = 218.4, 333.4$ and $443.7 \text{ kg}/(\text{m}^2 \cdot \text{s})$ at $\Delta T_{\text{sub}} = 4.9^\circ\text{C}$ and $P = 652 \text{ kPa}$. As shown in Fig. 5(b), the effect of mass flux on the ONB is similar to the effect of subcooling. The heat transfer coefficient of single phase convection decreases with the decrease in the mass flux. Therefore, the heated wall cannot be fully cooled, and the wall superheat is more likely to reach the critical value which is essential for the bubble nucleation. As a result, the heat flux and wall superheat at the ONB are higher for the large mass flux.

The effect of the pressure on the ONB is illustrated in Fig. 5(c). The pressure increases from 450 to 850 kPa for an operating condition of $\Delta T_{\text{sub}} = 4.7^\circ\text{C}$ and $G = 222.8 \text{ kg}/(\text{m}^2 \cdot \text{s})$ in No. 1 coil at the cross-section of $\alpha = 270^\circ$. Note that the superheat and heat flux of the ONB decrease with the increase in inlet pressure. This is mainly due to the fact that the surface tension of R134a is lower in the high pressure region, resulting in the liquid much more easily fully flooding the pits and thus enhancing the bubble formation. Meanwhile, a similar phenomenon is also noted by Chen et al.^[12].

The effects of the geometrical parameters on the ONB are illustrated in Fig. 6. First, the effect of the helical pitch on the ONB is shown in Fig. 6(a) with $d_p = 120, 80$ and 40 mm for an operating condition of $G = 221.7$

$\text{kg}/(\text{m}^2 \cdot \text{s})$, $\Delta T_{\text{sub}} = 9.9^\circ\text{C}$ and $P = 651 \text{ kPa}$. The results indicate that the pitch of the helical coil has a rather slight effect on the boiling curves. Next, the effect of coil diameter on the ONB is tested at the cross-section of $\alpha = 45^\circ$ for $G = 219.1 \text{ kg}/(\text{m}^2 \cdot \text{s})$, $\Delta T_{\text{sub}} = 10.0^\circ\text{C}$ and $P = 651 \text{ kPa}$. It can be seen from Fig. 6(b) that the higher superheat and heat flux are needed to achieve the ONB in the helical coil with smaller coil diameter, but the temperature undershoot is nearly the same. On the one hand, the heated length between the inlet and test position of $\alpha = 45^\circ$ is shorter for $D_c = 220 \text{ mm}$ so that the local subcooling is higher for the smaller diameter coil. On the other hand, the effect of secondary flow for the smaller diameter coil is more obvious than that in the larger diameter coil so that the heat transfer is enhanced in the smaller diameter coil. Therefore, the superheat and heat flux of the ONB are higher for the coil of $D_c = 220 \text{ mm}$.

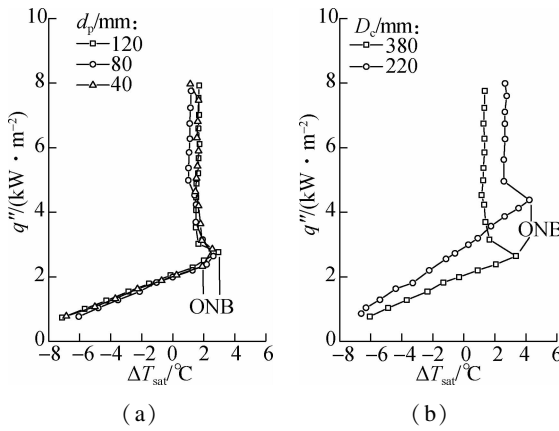


Fig. 6 Dependence of the ONB on geometrical parameters. (a) Helical pitch; (b) Coil diameter

2.3 Correlation equations for the ONB

A number of correlations for predicting the heat flux at the ONB were proposed for the conventional channels^[1-6]. Based on the minimum superheat criterion, Sato and Matsumura^[13] analytically proposed a correlation for expressing the heat flux at the ONB in terms of the wall superheat. The expression is given as

$$q''_{\text{ONB},s} = \frac{k_f i_{fg} \rho_v T_{\text{sat}}^2}{8\sigma T_{\text{sat}}} \quad (3)$$

where k_f is the thermal conductivity of the fluid; i_{fg} is the latent heat; ρ_v is the density of the vapor; and σ is the surface tension.

However, the existing correlations cannot be used for predicting the heat flux at the ONB for the helical coil due to the influence of geometrical construct and secondary flow in helical coil. Accordingly, the non-dimensional parameters are added to develop a new correlation for predicting the heat flux at the ONB for vertical helically-coiled tubes. Dean number ($Dn = Re(d_i/D_c)^{0.5}$) is the product of the Reynolds number ($Re = Gd/\mu$) and the square root of the curvature ratio. It is postulated that the

effects of the mass flux and curvature ratio on the ONB can be revealed by the Dean number. The density ratio (ρ_v/ρ_l) expresses the effect of the pressure on the ONB. Meanwhile, the inlet subcooling has an obvious effect on the heat flux at the ONB. The ratio of local subcooling and superheat ($\Delta T_{\text{sub}}/\Delta T_{\text{sat}}$) is introduced to describe the effect of the subcooling on the ONB.

The heat flux at the ONB can be defined as

$$q''_{\text{ONB}} = f\left(Dn, \frac{\rho_v}{\rho_l}, \frac{\Delta T_{\text{sub}}}{\Delta T_{\text{sat}}}, q''_{\text{ONB},s}\right) \quad (4)$$

Based on the experimental data, the correlation of heat flux at the ONB for vertical helically-coiled tubes obtained by means of multiple nonlinear regression analyses can be expressed as

$$q''_{\text{ONB}} = 9.61 \times 10^{-7} Dn^{0.76} \left(\frac{\rho_v}{\rho_l}\right)^{-1.66} \left(\frac{\Delta T_{\text{sub}}}{\Delta T_{\text{sat}}}\right)^{0.58} q''_{\text{ONB},s}^{0.91} \quad (5)$$

It is noted from Fig. 7 that 93.0% of the present experimental data for heat flux at the ONB can be correlated within $\pm 15\%$ by Eq. (5). The new correlation for heat flux at the ONB is applicable to the following range of parameters: $111 \leq Dn \leq 2626$, $1.7 \times 10^{-2} \leq \rho_v/\rho_l \leq 3.5 \times 10^{-2}$ and $0.04 \leq \Delta T_{\text{sub}}/\Delta T_{\text{sat}} \leq 3.18$.

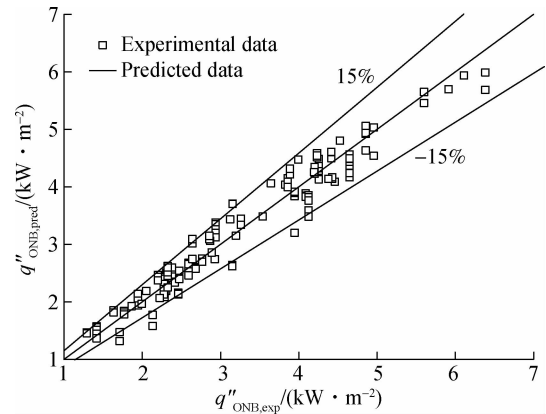


Fig. 7 Comparison between experimental and predicted q''_{ONB}

3 Conclusions

1) The angular position of the cross-section has a neglect effect on the heat flux at the ONB, but it has great effect on the superheat at the ONB.

2) The distribution of the superheat at the ONB is consistent with the temperature distribution of the single phase flow. As a result of subcooled boiling heat transfer, the temperature undershoots of the upper and lower sides are the largest and smallest in the circumference of the cross-section, respectively.

3) The wall superheat and heat flux at the ONB increase with the increase in mass flux and inlet subcooling, but decrease with the increase in system pressure and

helix diameter in vertical helically-coiled tubes. The helical pitch has a slight effect on the wall superheat and heat flux at the ONB.

4) A new correlation for predicting the heat flux at the ONB is developed by introducing the Dean number, density ratio and the ratio of subcooling and wall superheat in vertical helically-coiled tubes, and it agrees well with the experimental data.

References

- [1] Hsu Y Y. On the size range of active nucleation cavities on a heating surface[J]. *Journal of Heat Transfer*, 1962, **84**(3): 207–215. DOI:10.1115/1.3684339.
- [2] Kandlikar S G, Mizo V, Cartwright M, et al. Bubble nucleation and growth characteristics in subcooled flow boiling of water[C]// *National Heat Transfer Conference—ASME*. Baltimore, USA, 1997, **4**: 11–18.
- [3] Basu N, Warrier G R, Dhir V K. Onset of nucleate boiling and active nucleation site density during subcooled flow boiling[J]. *Journal of Heat Transfer*, 2002, **124**(4): 717–728. DOI:10.1115/1.1471522.
- [4] Zhao N, Zhang W, Yang L X. Subcooled boiling in narrow channels with different sizes[J]. *Journal of Chemical Industry and Engineering*, 2016, **67**(S1): 47–56. DOI: 10.11949/j.issn.0438-1157.20160641. (in Chinese)
- [5] Castiglione T, Pizzonia F, Piccione R, et al. Detecting the onset of nucleate boiling in internal combustion engines[J]. *Applied Energy*, 2016, **164**: 332–340. DOI: 10.1016/j.apenergy.2015.11.083.
- [6] Zhou Y L, Hou Y D, Li H W. Experiment study on onset of nucleate boiling in rod bundle channel[J]. *Atomic Energy Science and Technology*, 2014, **48**(8): 1416–1420. DOI:10.7538/yzk.2014.48.08.1416. (in Chinese)
- [7] Fsadni A M, Whitty J P M. A review on the two-phase heat transfer characteristics in helically coiled tube heat exchangers[J]. *International Journal of Heat and Mass Transfer*, 2016, **95**: 551–565. DOI:10.1016/j.ijheatmasstransfer.2015.12.034.
- [8] Santini L, Cioncolini A, Butel M T, et al. Flow boiling heat transfer in a helically coiled steam generator for nuclear power applications[J]. *International Journal of Heat and Mass Transfer*, 2016, **92**: 91–99. DOI:10.1016/j.ijheatmasstransfer.2015.08.012.
- [9] Kong L J, Han J T, Chen C N, et al. Subcooled flow boiling heat transfer characteristics of R134a in horizontal helically coiled tubes[J]. *Journal of Enhanced Heat Transfer*, 2015, **22**(4): 281–301. DOI:10.1615/jenh-heattransf.v22.i4.20.
- [10] Moffat R J. Describing the uncertainties in experimental results[J]. *Experimental Thermal and Fluid Science*, 1988, **1**(1): 3–17. DOI: 10.1016/0894-1777(88)90043-x.
- [11] McConalogue D J, Srivastava R S. Motion of a fluid in a curved tube[J]. *Proceedings of the Royal Society A: Mathematical, Physical and Engineering Sciences*, 1968, **307**(1488): 37–53. DOI:10.1098/rspa.1968.0173.
- [12] Chen C A, Chang W R, Li K W, et al. Subcooled flow boiling heat transfer of R-407C and associated bubble characteristics in a narrow annular duct[J]. *International Journal of Heat and Mass Transfer*, 2009, **52**(13/14): 3147–3158. DOI:10.1016/j.ijheatmasstransfer.2009.01.027.
- [13] Sato T, Matsumura H. On the conditions of incipient subcooled boiling with forced convection[J]. *Bulletin of Japan Society of Mechanical Engineers*, 1964, **7**(26): 392–398.

立式螺旋管内过冷沸腾起始点实验研究

孔令健¹ 韩吉田² 陈常念² 刘志刚¹

(¹ 山东省科学院能源研究所, 济南 250014)

(² 山东大学能源与动力工程学院, 济南 250061)

摘要:以 R134a 为工质, 对立式螺旋管内过冷沸腾起始点进行了实验研究. 实验参数范围为: 压力 450~850 kPa, 入口过冷度 4.7~15.0 °C, 热流密度 0.11~8.9 kW/m², 质量流量 218.2 to 443.7 kg/(m²·s). 对立式螺旋管内过冷沸腾起始点的热流密度、过热度和温度下降幅度进行了分析, 研究了质量流量、系统压力、入口过冷度和螺旋管几何参数对过冷沸腾起始点的影响. 实验结果表明: 过冷沸腾起始点的热流密度和过热度随着质量流量和入口过冷度的增大而增大, 但是随着系统压力和螺旋直径的增大而减小; 螺旋节距对过冷沸腾起始点的热流密度和过热度的影响很小. 基于实验数据提出了螺旋管内过冷沸腾起始点热流密度的关联式, 且该关联式的预测精度较高.

关键词: 两相流; 过冷沸腾; 沸腾起始点; 螺旋管

中图分类号: TK121